Journal of Nuclear Materials 386–388 (2009) 147–151

Contents lists available at ScienceDirect

Journal of Nuclear Materials

journal homepage: www.elsevier.com/locate/jnucmat

Dependence of steady-state radiation swelling rate of l 0.1C–16Cr–15Ni–2Mo–2Mn–Ti–Si austenitic steel on dpa rate and irradiation temperature

A.V. Kozlov *, I.A. Portnykh

FSUE 'Institute of Nuclear Materials', Zarechny 624250, Russia

A B S T R A C T

A large number of swelling measurement data on the 0.1C–16Cr–15Ni–2Mo–2Mn–Ti–Si austenitic steel used as a fuel cladding at temperatures 640–870 K in the BN-600 fast reactor were analyzed. It was found that within irradiation temperatures 690–830 K a steady-state swelling dose rate was from 0.45%/dpa to 1.1%/dpa. By the statistical model of point defect migration for the 0.1C–16Cr–15Ni–2Mo–2Mn–Ti–S steel the dependence of the steady-state swelling rate on the irradiation temperature and displacement rate was calculated. The calculation data were consistent with the experimental data.

1. Introduction

In order to predict vacancy swelling under high dose neutron irradiation for fission and fusion reactors it is needed to know both the condition of an onset of steady-state swelling and a steady-state swelling rate. One current concept [1] is that the steady-state swelling rate is ~1%/dpa independent of dpa rate and temperature over a wide range of typical neutron irradiation conditions. At the same time the different experimental data ranging from 0.8%/dpa to 1.6%/dpa [2] can be found in other publications. The objective of this paper is to explore the dependence of a steady-state swelling rate on an irradiation temperature and dpa rate.

2. Material and examination methods

Approximately 1800 swelling measurements on the 0.1C–16Cr–15Ni–2Mo–2Mn–Ti–Si steel as fuel cladding irradiated under temperatures from 640 to 870 K [3] in the BN – 600 reactor were analyzed for the dependence of a steady-state swelling rate. The measurements were made on 41 fuel claddings taken from 10 different fuel element assemblies. The first data set was obtained from 3 assemblies irradiated in the 750 mm-length core at a maximum dpa rate of 2×10^{-6} dpa/s. The second data set was obtained from 7 assemblies operated in the modernized core of 1030 mm-length at a maximum dpa rate of 1.6×10^{-6} dpa/s. The compositions of cladding materials before and after the core modernization were slightly different (Table 1).

The data of both sets were divided into groups, each corresponding to a 10 degree-interval of the irradiation temperatures. Irradiation temperatures inside such group were assumed to be the same to facilitate plotting the experimental dose dependencies of swelling.

These dependencies were described by the empirical equation [3] with the corrections that took into account the results provided in [4], they suggested that the onset of the steady-state followed a swelling value of ~10%. The approximation equation of the dose dependence on swelling was

$$S = 0, \quad \text{at} \quad D \le D_0, \tag{1}$$

$$S = A \times (D - D_0) \times (1 - \exp(-p \times (D - D_0))), \quad \text{at} \quad D_0 < D < D_s, \tag{2}$$

$$S = V_s \cdot (D - D_s) + S_s \quad \text{at} \quad D \ge D_s, \tag{3}$$

where V_s is the steady-state swelling dose rate, dpa^{-1}; D_0 is the incubation swelling dose, dpa; D_s is the dose corresponding to the onset of the steady-state swelling, dpa; p and A are the factors describing a rate of reaching the steady-state of swelling, dpa^{-1}; S_s is determined by Eq. (2) at $D = D_s$.

The factors in Eq. (2) were fitted using both the optimization by the criterion χ^2 [5] and the swelling values of <10%. For D_s the dose was chosen such that gave S_s = 10% from Eq. (2). Then the steady-state rate, V_s, was obtained from Eq. (3) by the points representing the swelling of >10% and the D_s-value. V_s can be estimated also from the tangent slope to the curve of Eq. (2) at D_s position (Fig. 1) and it can be considered as a lower estimate of steady-state rate. This procedure was considered correct for the temperature intervals, where the swelling value was not less than S_s.

The irradiation temperature range, that met the above conditions for data set #1, was 700–750 K, where maximal swelling values though reached but not exceeded S_s. For this range V_s was

* Corresponding author.
E-mail address: sfti@uraltc.ru (A.V. Kozlov).

0022-3115/$ - see front matter © 2009 Published by Elsevier B.V.
doi:10.1016/j.jnucmat.2008.12.072

Table 1
Composition of claddings made of 0.1C–16Cr–15Ni–2Mo–2Mn–Ti–Si steel.

Data set	Element, wt%												
	C	Cr	Ni	Mo	Mn	Si	Ti	V	B	N	Co	P	S
#1	0.06–0.07	15.5–16.7	14.7–15.1	2.18–2.44	1.0–1.8	0.41–0.47	0.35–0.46	–	0.002–0.005	0.005–0.014	0.010–0.020	0.012–0.017	0.004–0.005
#2	0.06–0.07	15.9–16.7	14.0–14.7	2.09–2.24	1.4–1.6	0.39–0.50	0.30–0.41	0.10–0.24	0.001–0.003	0.009–0.015	0.004–0.010	0.006–0.018	0.003–0.007

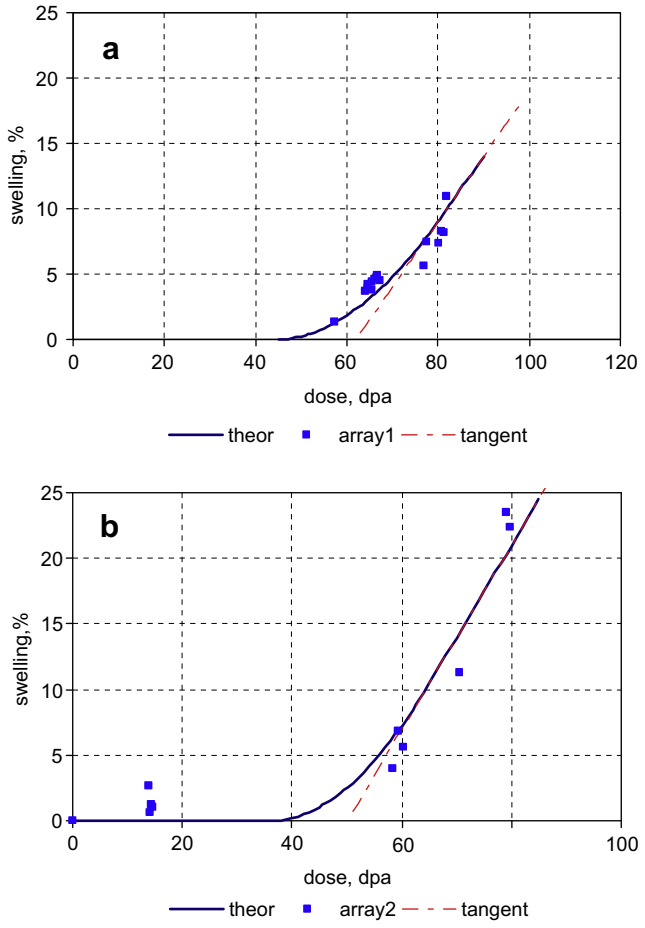

Fig. 1. Typical dose dependencies of swelling: (a) for data set #1, T_{irr} = 728 K; (b) for data set #2, T_{irr} = 718 K.

obtained only by the tangent slope technique. For data set #2 the dpa rate exceeded the value of D_s over the range 700–830 K. For the specimens chosen by the above criterion the dpa rates were 1.5–2.0 × 10^{-6} dpa/s for data set No. 1 and 1.0–1.6 × 10^{-6} dpa/s for data set #2.

3. Results

A typical shape of the dose dependencies of swelling obtained from the experiments (designated as squares) and that of the dependencies derived from Eqs. (1)–(3) (designated as lines) are shown in Fig. 1.

The steady-state swelling dose rates, V_s (%/dpa), found by the above procedure for different temperature ranges are given in Table 2. It includes the values obtained from Eq. (3) and those obtained by the tangent slope to the curve of Eq. (2) at the D_s position. For data set #1 the lower estimate of V_s is within 0.44–0.54%/dpa. For data set No. 2 V_s varies from 0.6%/dpa to1.1%/dpa. It is noted that the values of V_s obtained by the tangent slope technique are changing within narrower limits than the values obtained from

Table 2
Steady-state swelling dose rate of 0.1C–16Cr–15Ni–2Mo–2Mn–Ti–Si steel at different irradiation temperatures.

Irradiation temperature (K)	Steady-state swelling dose rate V_s		
	Data set No. 1	Data set No. 2	
	Tangent slope technique	Eq. (3)	Tangent slope technique
698	0.44	0.6	0.6
708	0.44	1.1	0.6
718	0.5	0.7	0.6
728	0.5	0.7	0.7
738	0.52	0.7	0.7
748	0.54	1.1	0.8
758		0.7	0.7
768		1	0.7
778		0.8	0.8
788		0.7	0.7
798		1	0.7
808		0.6	0.6
818		0.7	0.7
828		0.6	0.6

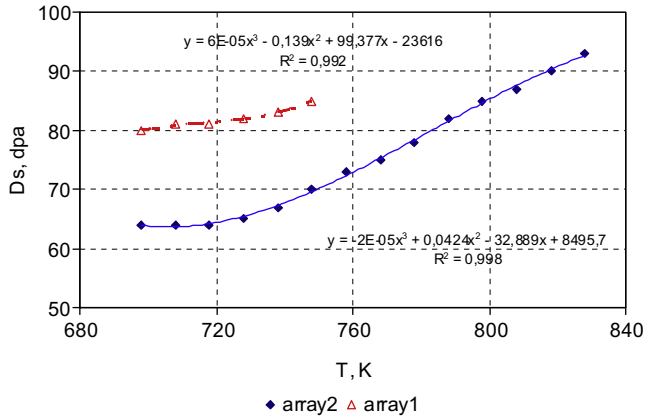

Fig. 2. Irradiation temperature dependence on dose D_S, corresponding to a steady-state swelling onset.

Eq. (3). The temperature dependencies of D_s for both data sets are shown in Fig. 2. They are well described by cubic polynomials.

4. Data analysis

The main instrument of the analysis was the statistical thermodynamic model of an irradiation-induced [6] point defects migration to sinks. This model allows to determine the mean time of diffusion of vacancies and interstitials to reach the sinks of different types. The mean time is expressed through the part of the volume occupied by the areas adjacent to the sinks. The model also characterizes a mobility of the point defects and their interactions with the sinks. In order to determine a swelling rate one needs to know a flow of vacancies and interstitials into voids and to take into account a flow of vacancies emitting from the voids.

When a surface of voids is well developed absorption of point defects by the voids makes an essential contribution to a total balance of vacancies and interstitials in a crystal. In this case the point defect balance equation must comprise the term of the point defect absorption by voids in addition to the terms of the absorption by grain boundaries, dislocations and recombination. The most easy for such calculation is the case when a total surface area of the voids does not change and that case is realized at the stationary swelling stage [4]. The volume of the area adjacent to a void of a diameter $\boldsymbol{d}$ is determined by the formulae

$$\Delta V = \pi \cdot a \cdot (d^2 + 2d \cdot a + 4a^2/3), \tag{4}$$

where $\boldsymbol{a}$ is the lattice parameter and $\boldsymbol{d}$ is the void diameter. According to [6] in the approximation of the voids of the same mean-square size the expression of mean diffusion time for vacancies to reach the voids is

$$\tau_{vv} = \frac{1}{\nu \cdot \pi \cdot n \cdot a \cdot (d^2 + 2d \cdot a + 4a^2/3)} \cdot \exp\left(\frac{E_{mv}}{kT}\right) \cdot \left(1 + 5 \cdot \exp\left(-\frac{E_v - U}{kT}\right)\right), \tag{5}$$

where E_{mv} is the energy of vacancy migration; E_v is the energy of vacancy formation; k is Boltsman constant; T is the temperature; n is the concentration of voids; ν is Debay frequency; U is determined as

$$U = \frac{a^3 \cdot \gamma}{d}, \tag{6}$$

where γ is the surface tension coefficient.

The time of diffusion (5) is readily expressed through the total surface area of voids as

$$F = \pi \cdot n \cdot d^2, \tag{7}$$

where n is the concentration of voids. A mean-square diameter of pores in the 0.1C–16Cr–15Ni–2Mo–2Mn–Ti–Si steel at steady-state stage over the range 690–830 K takes the values from 20 to 80 nm [7]. Herewith the energy U changes from 4×10^{-2} to 4.5×10^{-3} eV, that is negligibly small as compared to the energy of vacancy formation. The vacancy formation energy itself converts the exponent in the second term in brackets into a value ranging from 3×10^{-12} to 4×10^{-8}, that is substantially less than 1. Besides, $a/d \ll 1$. A time of diffusion of interstitials (with their energy of migration) into voids, τ_{iv}, is calculated in the same manner. Taking into account these approximations Eq. (5) is expressed as

$$\tau_{(v,i)v} = \frac{1}{\nu \cdot F \cdot a} \cdot \exp\left(\frac{E_{m(v,i)}}{kT}\right) \tag{8}$$

Thus, the balance equations set for the stationary (equilibrium in irradiation conditions) concentration of point defects [6] is

$$\delta \cdot G + G_{termv} = \left(\frac{3}{R_b \cdot (1+5 \cdot \exp(-E_{vb}/kT))} + \frac{3 \cdot \pi \cdot \rho_d \cdot a}{2 \cdot (1+5\exp(-E_{vd}/kT))} + F\right) \cdot a \cdot \nu \cdot c_v \cdot \exp\left(-\frac{E_{mv}}{kT}\right) + \frac{16\pi \cdot 4\eta^3 \cdot c_i \cdot c_v \cdot \nu}{3} \cdot \exp\left(-\frac{E_{mi}}{kT}\right) \tag{9}$$

$$\delta \cdot G = \left(\frac{3}{R_b \cdot (1+5 \cdot \exp(-E_{ib}/kT))} + \frac{\pi \cdot \rho_d \cdot a}{2 \cdot (1+5\exp(-E_{id}/kT))} + F\right) \cdot \nu \cdot a \cdot c_i \cdot \exp\left(-\frac{E_{mi}}{kT}\right) + \frac{16\pi \cdot \eta^3 \cdot c_i \cdot c_v \cdot \nu}{3} \cdot \exp\left(-\frac{E_{mi}}{kT}\right), \tag{10}$$

where δ is the cascade efficiency; indices v, i are for vacancies and interstitials; c_v, c_i are the stationary concentrations of vacancies and interstitials, respectively; η is the radius of spontaneous recombination expressed as lattice parameters; E_{vd}, E_{id} are the energy of relation of a vacancy and an interstitial with the dislocation, respectively; E_{vb}, E_{ib} are the energy of relation of a vacancy and an interstitial with the grain boundary, respectively; R_b is a half of mean-grain size; ρ_d is the density of dislocations, G is the radiation damage rate; G_{term} is the term, which describes the intensity of thermal emission of vacancies from the grain boundaries, dislocations and voids, this term in the above approximation is expressed as

$$G_{termv} = \exp\left(-\frac{E_v + E_{mv}}{kT}\right) \cdot \nu \cdot a \cdot \left(\frac{3}{R_b \cdot (1 + 5 \cdot \exp(-E_{vb}/kT))} + \frac{\pi \cdot \rho_d \cdot a}{2 \cdot (1 + 5 \cdot \exp(-E_{vd}/kT))} + F\right), \tag{11}$$

The interactions of the point defects with impurities and second phase precipitates were not considered at this stage of calculations.

The analytical solutions of the system of Eqs. (9) and (10) were obtained and the dependencies of c_v, c_i on the irradiation temperature, displacement rates and the steel characteristics were calculated. For these equations temperature variations were over the range 573–823 K, the displacement rate was from 10^{-2} to 10^{-9} dpa/s and the data on the 0.1C–16Cr–15Ni–2Mo–2Mn–Ti–Si structure as well as point defects in the steel exhibited in Table 3 were used. The structure characteristics were determined experimentally for the specimens related to data set No. 2, the values of the point defect migration energy were taken from [8], the energy of point defect interaction with dislocations were estimated by the model suggested in [9] with the assumption that the dislocations are of the SD-type as given in Table 4 [9]; the values of the total surface area of the voids at different temperatures at the steady- state swelling were provided in [7] and the cascade efficiency was taken from [10].

The dependencies of the stationary concentration of vacancies and interstitials at the steady-state swelling on a dpa rate for different irradiation temperatures are shown in Fig. 3(a) and (b). At 823 K the concentration of vacancies does not change with an increase in the dpa rate to 10^{-7} dpa/s and keeps thermal stability. The swelling does not occur under these conditions. A further increase in the dpa rate leads to slow (weakly detectable in logarithmic coordinates) growth of the stationary concentration of vacancies followed by its faster increase (Fig. 3(a)). At lower temperatures the increase in the vacancy concentration begins at lower dpa rates. The stationary concentration of interstitials over the whole temperature range of examination substantially exceeds thermally equilibrium values ($\sim 2 \times 10^{-25}$ m^{-3} at 823 K) and at temperatures higher than 673 K the temperature dependence is very weak (Fig. 3(b)).

Using the obtained values of stationary concentrations of vacancies and interstitials and the expression of the mean diffusion time (8), the expressions for both a flow of vacancies and interstitials into voids and a flow out of pores can be derived. Then the swelling rate at the stationary stage can be calculated from these expressions

$$\dot{S}_s = J_{v+} - J_{i+} - J_{v-} = \frac{c_v}{\tau_{vv}} - \frac{c_i}{\tau_{iv}} - \nu \cdot a \cdot F \cdot \exp\left(-\frac{E_v + E_{mv}}{kT}\right), \tag{12}$$

where J_{v+}, J_{i+} are the flows of vacancies and interstitials into voids; J_{v-} is the flow of vacancies emitting from voids; $\dot{S}_s$ is the swelling rate at the stationary stage, s^{-1}. We substitute the mean diffusion time expressions (8) in (12) and obtain

$$\dot{S}_s = \nu \cdot F \cdot a \cdot \left(\left(c_v - \exp\left(-\frac{E_v}{kT}\right)\right) \cdot \exp\left(-\frac{E_{mv}}{kT}\right) - c_i \cdot \exp\left(-\frac{E_{mi}}{kT}\right)\right), \tag{13}$$

where F is the integral square of the voids surface determined by experimental porosity measurements in [7]. In order to find the dpa rate in %/dpa, one needs to multiply a value of $\dot{S}_s$ (calculated by (13) by $100/G$.

Table 3
Structure characteristics of the 0.1C–16Cr–15Ni–2Mo–2Mn–Ti–Si steel as fuel cladding in BN-600 reactor.

Value	a (m)	R (m)	ρ_d (m^{-2})	η	E_{mv} (eV)	E_m(eV)	ν (c^{-1})	δ
Magnitude	3.6×10^{-10}	5×10^{-6}	3×10^{14}	1	1.23	0.3	1×10^{13}	0.3

Table 4
The edge dislocations, that are the most energy – contributing to f.c.c. metals, and their energies of binding with an interstitial in the <100> dumbbell configuration and with a vacancy.

Designation of dislocation	Burger's vector, ***b***	Plane of sliding	Direction of dislocation, ξ	Binding energy in f.c.c. iron (eV)	
				Interstitial	Vacancy
SD	a/2[110]	(111)	[110]	0.96	0

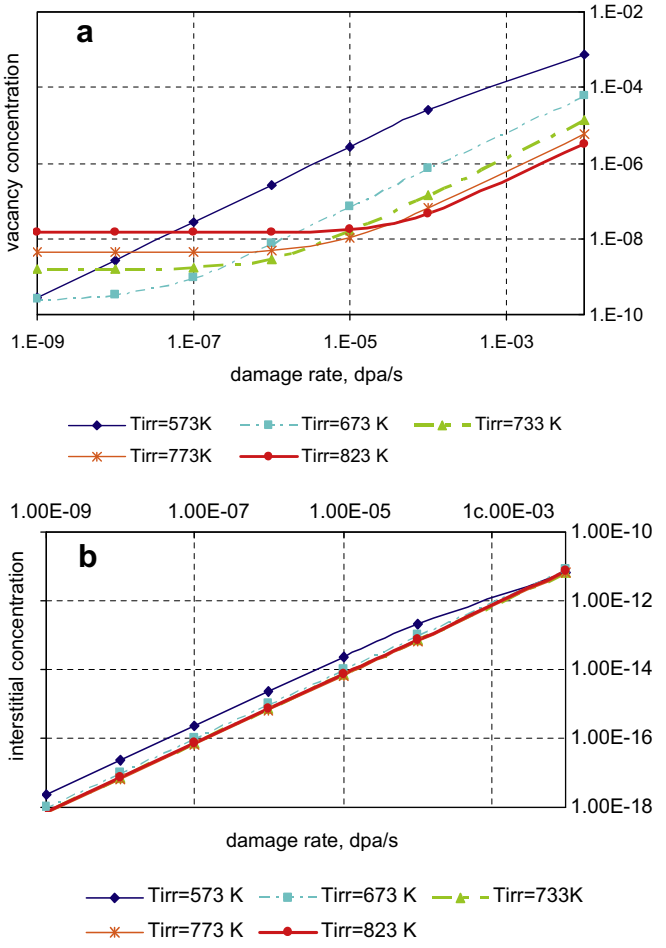

Fig. 3. Dependencies of stationary concentration of vacancies (a) and interstitials (b) at the steady-state swelling on dpa rate at different irradiation temperatures.

We should note that all the values in the calculation formulas (for concentration of vacancies and interstitials, concentration of voids, dislocation density, specific grain boundary area and etc.,) have to be normalized by a unit volume of matrix rather than a volume unit of body, (i.e., a volume of voids present in a cubic meter has to be deducted).

The data on the temperature dependence of the steady-state swelling rate at 1×10^{-6} dpa/s, calculated by (13) are plotted in

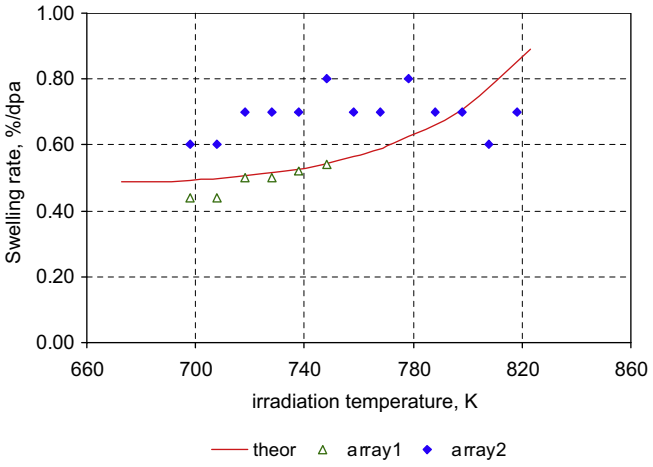

Fig. 4. Temperature dependence of steady-state swelling rate: calculated for dpa rate 1×10^{-6} dpa/s (line); experimental results for data set #1 (triangles); experimental results for data set #2 (rhombs).

Fig. 4 (line). This figure also includes the values (Table 2) determined from the experiment for data set #1 (triangles) and for data set #2 (rhombs).

It is seen from the figure that most of the experimental data of set #2 (the structure characteristics from it were used in the calculation) are located somewhere higher than the calculation values and they have a large scattering, with which the temperature dependence is not so evident. In the experimental data of set #1, where the scattering is essentially less, the tendency of the steady-state rate to grow with an irradiation temperature can be noticed. The theoretical dependence in Fig. 4 was plotted without accounting for the interaction of point defects with impurities and second phase precipitates and therefore an absolute value of steady-state rate could not be obtained from it. Since not a single fitting parameter has been used in the theoretical calculations, we can state that in general the calculation values are in a good agreement with the experimental data. Some discrepancy can be noted in the run of the calculation dependence curve and the experimental data of set #2 at temperatures higher than 800 K. It can be attributed to a scarce amount of the experimental data on swelling exceeding 10% at these temperatures, hence the experimental estimation of the swelling rate value may be inaccurate.

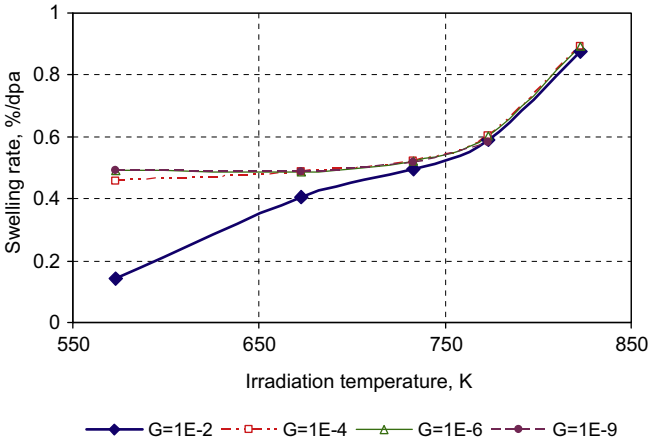

Fig. 5. Temperature dependence of steady-state swelling rate at different dpa rates from 1×10^{-2} to 1×10^{-9} dpa/s.

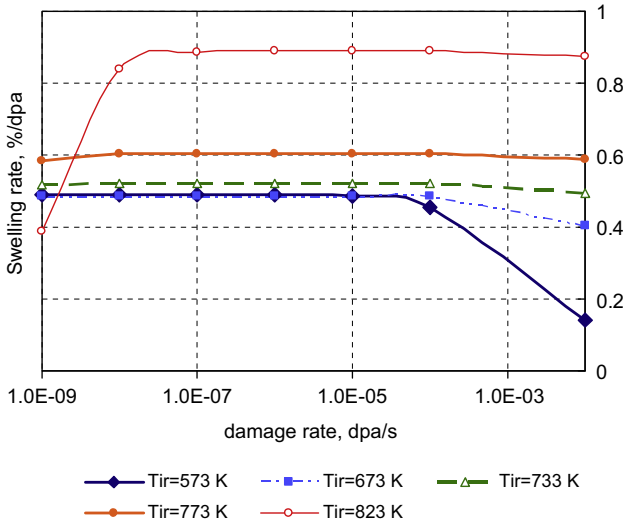

Fig. 6. Dependence of steady-state swelling rate on dpa rates at different irradiation temperatures from 573 to 823 K.

The suggested calculation technique was used to analyze the manner of the dependence of steady-state swelling dpa rate on irradiation temperature and displacement rate. Fig. 5 shows the dependencies of stationary swelling rate on irradiation temperature at dpa rates over the range 1×10^{-2} to 1×10^{-9} dpa/s. It is seen that at temperatures from 573 to 750 K and dpa rates lower than 10^{-4} dpa/s the stationary swelling rate practically does not depend on temperature. A further increase of the temperature leads to a growth of the swelling rate. At higher dpa rates ($>10^{-4}$ dpa/s) the steady-state rate increases monotonously with temperature (in the examined range).

The dependence of steady-state rate on dpa rates at different irradiation temperatures over the range 573–823 K is presented in Fig. 6. It shows that the stationary swelling rate does not depend on the dpa rate at all irradiation temperatures within the examined range of dpa rates from 1×10^{-8} to 1×10^{-4} dpa/s.

5. Conclusions

- The experimental values of steady-state swelling dpa rates from 0.45%/dpa to 1.1%/dpa were obtained for the 0.1C–16Cr–15Ni–2Mo–2Mn–Ti–Si steel as fuel cladding material irradiated at 700–830 K in the BN-600 fast reactor.
- The stationary swelling rate for the specimens in two sets with slightly different content differs by a factor of ~1.5.
- The temperature dependence of the steady-state swelling rate was calculated by the statistical model of point defect migration for the 0.1C–16Cr–15Ni–2Mo–2Mn–Ti–Si steel, this dependence is consistent with the experimental data obtained at temperatures lower than 800 K.
- The calculations made by the model show that at the dpa rates lower than 10^{-4} dpa/s over the range 570–730 K the stationary swelling rate does not change and at higher irradiation temperatures the steady-state swelling rate increases with temperature. The stationary swelling rate at all irradiation temperatures does not depend on dpa rates over the range 10^{-8}–10^{-4} dpa/s.

References

[1] F.A. Garner, Nucl. Mater. 10A (1996) 419 (Chapter 6) Part 1.
[2] V.S. Neustroyev, V.N. Golovanov, N.M. Mitrofanova, V.K. Shamardin, A.V. Povstyanko, M.G. Bogolepov, V.A. VANT ser.: Phys. Radiat. Defects Radiat. Mater. Sci. (FRP & RM), Issues 1(4) 2(5) (1989) 3.
[3] A.V. Kozlov, I.A. Portnykh, S.V. Bryushkova, E.A. in: M.L. Grossbeck (Ed.), Effects of Radiation on Materials, Adaksdngkasnd, Springer, West Coshohocken, PA, 2004, p. 446.
[4] A.V. Kozlov, I.A. Portnykh, Met. Phys. Mater. Sci. 103 (1) (2007).
[5] V.E. Gmurman, Theory of probability and mathematical statistics, M.: Vyshaya shkola (2001) 479.
[6] A.V. Kozlov, Met. Phys. Mater. Sci., submitted for publication.
[7] I.A. Portnykh, A.V. Kozlov, VANT ser.: Mater. Sci. New Mater., submitted for publication.
[8] A.V. Kozlov, E.N. Shcherbakov, L.A. Skryabin, I.A. Portnykh, Phys. Chem. Mater. Treat. 1 (2006) 9.
[9] N.A. Dubasova, A.B. Sivak, V.M. Chernov, Mater. Sci. New Mater. Issues 1(66) (2006) 233.
[10] Yu.N. Devyatko, A.A. Plyasov, S.V. Rogozhkin, V.M. Chernov, VANT ser.: Mater. Sci. New Mater. 1 (66) (2006) 31.